Revised version submitted to Angewandte Chemie. Different from the finally published version. May contain formatting, typographical and other errors.

Unexpected role of hyaluronic acid in trafficking siRNA across cellular barrier: First biomimetic, anionic, non-viral transfection method

Maruthibabu Paidikondala,[a] Vignesh Kumar Rangasami,[b] Ganesh N. Nawale,[a] Tommaso Casalini,[c,d] Giuseppe Perale,[c] Sandeep Kadekar,[a] Gaurav Mohanty,[e] Turkka Salminen,[f] Oommen P. Oommen,[b] and Oommen P. Varghese*[a]*

Abstract: *Circulating nucleic acids such as short interfering RNA (siRNA), microRNA and long non-coding RNAs regulate multiple biological processes; however, the mechanism by which these molecules penetrate target cell is poorly understood. We present a new concept on the role of extracellular matrix (ECM) derived polymers in binding siRNA and trafficking them across the plasma membrane. Our thermal melting, dynamic light scattering (DLS), scanning electron microscopy (SEM) and computational analysis indicate that hyaluronic acid (HA), an ECM component, can stabilize siRNA by hydrogen bonds as well as by Van der Waals interactions. Such stabilization facilitated HA size and concentration-dependent gene silencing in CD44 positive human osteosarcoma cell line (MG-63) as well as human mesenchymal stromal cells (hMSCs) but not so efficiently in low-CD44 expressing human breast cancer cells (MCF-7). The cell surface CD44 mediated siRNA uptake was validated by receptor blocking experiments. Our native HA-based siRNA transfection represents the first report on anionic, non-viral delivery method that resulted in ~60% gene knockdown in both the cell types and correlated with a reduction in protein translational levels.*

There are several non-coding RNAs such as small interfering RNA (siRNA), microRNA (miRNA), piwi-interacting RNA (piRNAs) and small nucleolar RNAs (snoRNAs) that are found in biological fluids and are known to be key gene modulators in eukaryotes.[1] The presence of extracellular nucleic acids in biological fluids was first reported in 1948.[2] Since then, significant effort has been made to unravel the role of these nucleic acids in maintaining steady-state or disease conditions. Even though the presence and function of such molecules are explored for therapeutic and diagnostic purposes, the mechanism of bidirectional transport of such molecules between cells, tissues and plasma is poorly understood.

Since nucleic acids have very limited stability under physiological conditions, it is believed that such molecules are protected by specific proteins such as Ago2 in the biological fluids or are encapsulated in the microvesicles produced by the cells.[3] There is also evidence of naked miRNAs in biological fluids such as in blood, urine, saliva and other body fluids, which forms the basis of their diagnostic applications.[4] Nevertheless, it is poorly understood how these sensitive molecules survive the hostile conditions in biological fluids and penetrate target tissues.[5] A deeper understanding of this intrinsic mechanism will immensely help to design biomimetic delivery systems that could efficiently transport such therapeutic molecules across cellular barriers. It is known that carbohydrates can stabilize nucleic acids through hydrogen bonding as well as by CH-π interactions.[6] The hydroxyl and amide groups present in carbohydrates form hydrogen bonds with bidentate phosphate groups which are placed in close proximity.[7],[8] The CH-π interactions were generally observed between the nucleobase and the nonpolar hydrogen atom of the carbohydrate.[6] However, an association of RNA molecules with negatively charged GAGs are not anticipated as they are expected to display strong electrostatic repulsion.

In this study, we have discovered a relatively unknown hitchhiking route to deliver short RNA molecules facilitated by hyaluronic acid (HA), a non-sulfated GAG present in the extracellular matrix. We performed a systematic analysis of HA-siRNA interactions using different sizes and concentrations of the HA polymer. We have previously reported that high molecular weight HA, although bind to the cell-surface CD44 receptors they are only taken up upon enzymatic cleavage to lower molecular weights.[9]

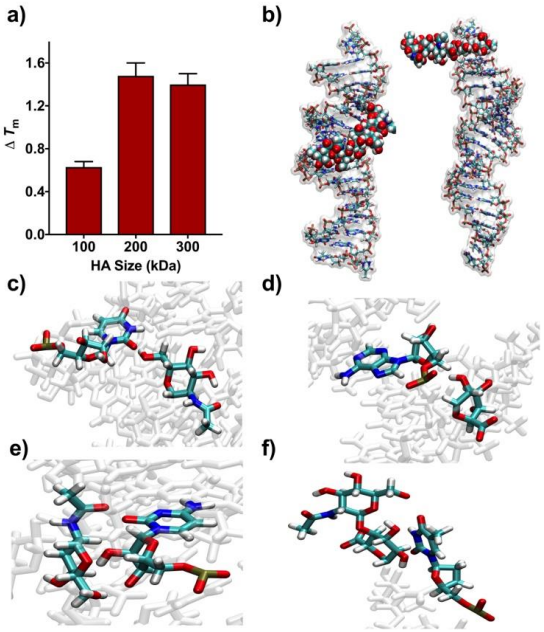

Figure 1. HA and siRNA interactions analyzed using thermal stability assay and computational assay. **a)** Thermal stability of siRNA with the different sizes of HA (100, 200 and 300 kDa) in PBS saline. **b)** Representative binding poses of HA along the phosphate backbone and the overhang. **c, d)** Details of hydrogen bonding interactions between HA and siRNA. **e)** Nonpolar contacts between HA and siRNA. **f)** CH-π interactions between HA and siRNA.

To study the plausible interaction between HA-siRNA and its effect on siRNA duplex thermal stability, we performed UV-melting studies in phosphate buffer. These experiments revealed that the unmodified HA exhibited effective stabilization of *anti-GAPDH* siRNA duplexes and such effects were dependent on the size of HA used and the salt concentration in the buffer (Figure 1a, S1). When duplex melting experiments were performed under

[a] M. Paidikondala, G. N. Nawale, [+] S. Kadekar, O. P. Varghese, Translational Chemical Biology Laboratory, Department of Chemistry, Ångström Laboratory, Uppsala University, 751 21, Uppsala, Sweden. E-mail: oommen.varghese@kemi.uu.se
[b] V. K. Rangasami, [+] O. P. Oommen, Bioengineering and Nanomedicine Lab, Faculty of Medicine and Health Technologies and BioMediTech Institute, Tampere University, Korkeakoulunkatu 3, Tampere-33720, Finland, Email:oommen.oommen@tut.fi
[+] These two authors made equal contribution to this paper.
[c] T. Casalini, G. Perale, Institute of Mechanical Engineering and Material Engineering, Department of Innovative Technologies, SUPSI, 6928, Manno, Switzerland.
[d] T. Casalini, Institute for Chemical and Bioengineering, Department of Chemistry and Applied Biosciences, ETH Zurich, 8093, Zurich, Switzerland.
[e] G. Mohanty, Materials Science and Environmental Engineering, Faculty of Engineering and Natural Sciences, Tampere University.
[f] T. Salminen, Tampere Microscopy Center, Tampere University.

Supporting information for this article is given via a link at the end of the document.

physiological condition (phosphate buffer saline or PBS, pH 7.4), a significant stabilization of duplex was observed with all sizes of HA tested as determined by the change in melting temperature (T_m) with respect to the naked siRNA (ΔT_m = 0.6 °C to ~1.5 °C; Figure 1a). We observed a maximum stabilization of siRNA duplex in case of 200 kDa HA (ΔT_m = 1.48 °C). Further increases in the size of HA (300 kDa) did not show any significant difference (ΔT_m = 1.40 °C), however a reduction in size (100 kDa) showed a drop in T_m (ΔT_m = 0.63 °C). To investigate this further, we performed melting experiments in PBS with lower salt concentration or with phosphate buffer without any salt. When the RNA was suspended in phosphate buffer containing low or no salt, we observed a marginal increase in duplex thermal stability (stabilization in ΔT_m = 0.6 °C – 0.4 °C). The lower ΔT_m values indicate that the amount of the salt plays an important role in minimizing the ionic repulsion between HA and siRNA and promoting the hydrogen bonding and CH-π interactions (Figure S1).

In order to elucidate the mechanism of this unique interaction between siRNA and HA that overcome the strong electrostatic repulsion, we performed computational analysis. We have recently demonstrated that subtle changes in the ionic state of HA affect molecular interactions with large proteins such as recombinant human bone morphogenetic protein-2 (rhBMP2).[10] We adopted a similar model system to identify the binding parameters between the double-stranded siRNA sequence and HA (*i.e.* RNA fragment interacting with a small HA oligomer composed of six units) from a theoretical point of view by means of molecular dynamics (MD) simulations. An exhaustive overview of the computational protocol is presented in the supporting information. Briefly, twelve guess complex structures were obtained through molecular docking (where major groove, minor groove and overhangs were considered potential binding sites) and used as input for MD simulations. The employed model system allowed us to rationalize the main mechanisms behind siRNA-HA binding. Our model results indicate that the main binding sites of RNA are the phosphate backbone and the overhangs (Figure 1b), which participate in forming hydrogen bonds (Figure 1c-d); nonpolar contacts between hydrophobic patches of carbohydrate rings (for backbone, Figure 1e) and CH-π interactions (for overhangs, Figure 1f). The interaction energies values ΔE_{int} along with specific contributions are reported in Table 1 for the most relevant binding poses.

Table 1. Most relevant binding poses and interaction energies of HA and siRNA.

Binding area	ΔE_{ele} [kcal mol^{-1}] [a]	ΔE_{VdW} [kcal mol^{-1}] [b]	ΔE_{Hbond} [kcal mol^{-1}] [c]	$\Delta\Delta G_{solv}$ [kcal mol^{-1}] [d]	ΔE_{int} [kcal mol^{-1}] [e]
Backbone	482.10 ± 20.32	-53.96 ± 4.82	-8.12 ± 2.70	-455.56 ± 18.36	-27.43 ± 4.89
Backbone	438.86 ± 20.32	-42.53 ± 5.24	-6.36 ± 2.80	-414.85 ± 15.81	-18.52 ± 4.96
Backbone	434.10 ± 7.89	-52.99 ± 4.31	-10.26 ± 3.56	-410.62 ± 7.34	-29.46 ± 4.20
Overhang	360.10 ± 14.29	-44.49 ± 5.85	-5.37 ± 2.24	-340.79 ± 13.24	-25.14 ± 5.61
Overhang	338.43 ± 15.44	-29.19 ± 2.97	-3.41 ± 1.62	-321.30 ± 14.09	-12.07 ± 2.90
Overhang	437.20 ± 4.92	-36.67 ± 4.92	-5.29 ± 2.32	-414.28 ± 19.76	-13.76 ± 3.92

Interaction energies and specific contributions for the most relevant binding poses. Values are expressed as an average ± standard deviation. [a] Electrostatic interactions. [b] Van der Waals interactions. [c] Hydrogen bonds. [d] Solubility of compounds. [e] Hydrophobic interactions.

As expected, electrostatic interactions ΔE_{ele} are unfavourable (positive values) because of the repulsion between negative charges, while favourable Van der Waals interactions ΔE_{VdW} (which account for nonpolar contacts and CH-π interactions) and hydrogen bonds ΔE_{Hbond} stabilize the complex. In addition, complexation increases the solubility of the compounds (negative $\Delta\Delta G_{solv}$) since hydrophobic patches are masked to the solvent, while charged and hydrophilic moieties are still accessible to water.

We have previously demonstrated that GAGs present in the extracellular matrix such as HA and chondroitin sulfate promote CD44-receptor-mediated endocytosis and could be used to deliver small molecule drugs[11] as well as DNA nanoparticles.[12] The siRNA duplex stabilization by HA prompted us to evaluate the functional aspect of the siRNA in a eukaryotic system. We, therefore, performed proof-of-concept experiments by silencing *signal transducer and activator of transcription 3* (*STAT3*) in human osteosarcoma cell line MG-63, a CD44 positive cell type.[13] In cancer cells, *STAT3* plays a vital role in cancer development by influencing cell proliferation, invasion, migration, angiogenesis, and metastasis.[14] There is currently an ongoing Phase II clinical trial using an antisense *STAT3* drug AZD9150 in patients with advanced pancreatic, non-small cell lung cancer, and mismatch repair deficient colorectal cancer.[15]

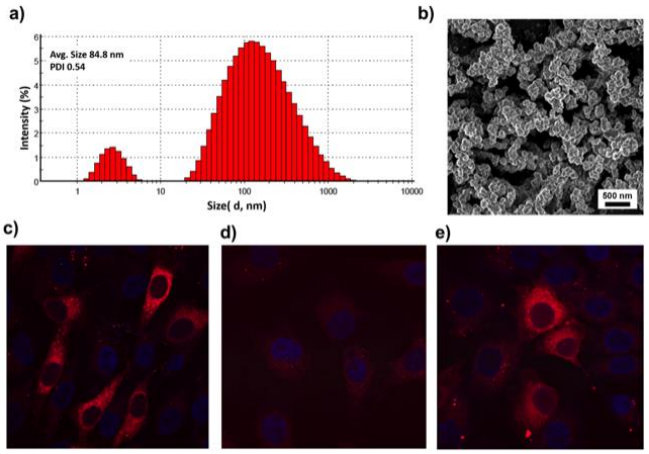

Figure 2. HA and siRNA interactions analyzed using DLS, SEM and microscopic analysis. **a)** DLS light scattering histogram demonstrating self-assembly of *anti-STAT3* siRNA with 200 kDa HA forming ~85 nm nanoparticles. **b)** SEM micrograph image indicating interactions between native HA and siRNA. **c)** Confocal microscopic image illustrating HA based cellular delivery of Cy3-labelled *anti-GAPDH* siRNA (red dots) in CD44 expressing MG-63 cells, **d)** almost no distribution of Cy3-labelled *anti-GAPDH* siRNA in CD44 blocked MG-63 cells and **e)** RNAiMAX based cellular delivery of Cy3-labelled *anti-GAPDH* siRNA (red dots) in CD44 expressing MG-63 cells.

In order to validate the unusual interactions between two negatively charged biopolymers (siRNA and HA) we performed the dynamic light scattering (DLS) studies, scanning electron microscope (SEM) studies and gel mobility shift assay (Figure 2a, 2b and S2). Surprisingly, DLS studies revealed an association of 200 kDa HA and siRNA forming a bimodal particle of ~85 nm with broad distribution (Figure 2a). Native HA and siRNA alone did not show any association in PBS. Similarly, the SEM analysis also revealed the association of the two biomolecules forming self-assembled nanoparticles below 100 nm (Figure 2b and S3 in SI). On the contrary, SEM images of HA dispersed in PBS did not show any particle formation (Figure S3). To further ascertain this unusual interaction, we performed the gel shift assay to determine the interaction between the polymers using agarose gel electrophoresis. Interestingly, we observed a visible retardation in mobility as a result of HA-siRNA interaction (Figure S2a-b). The observed mobility shift was however, lower than anticipated as unlike with cationic polymers, complexation with two anionic polymers is expected to migrate in the same direction (anode). Nevertheless, the thermal melting, gel shift, DLS and the SEM studies together with the computational analysis unequivocally

suggest an association between two anionic biomolecules. To further visualize the localization of siRNA intracellularly, we performed confocal microscopic studies with Cy3-labelled siRNA in MG-63 cells. The confocal images of MG-63 cells clearly indicated cytosolic distribution of siRNA with HA based and RNAiMAX based delivery (Figure 2c and 2e). However, no significant localization of Cy3-labelled siRNA was observed in CD44 blocked MG-63 cells (Figure 2d). Taken together, these findings clearly suggest a cell-surface CD44 receptor mediated delivery of siRNA.

To perform *in vitro* experiments, we selected 200 kDa HA and performed a dose-dependent experiment from 6.3 μM to 192 μM (HA concentrations were determined with respect to the disaccharide repeat units) using 200 nM anti-*STAT3* siRNA. As a positive control, we used commercially available reagent RNAiMAX. Quantitative RT-PCR results revealed an HA-dose dependent gene silencing with 64 μM concentration being the optimal (~55% knockdown or KD; Figure 3a). Further increment in HA concentration resulted in a decrease in transfection efficiency. We further evaluated the effect of HA-size on transfection as our melting studies indicated that HA size influences RNA duplex stability (Figure 3b). We, therefore, tested 100, 200, and 300 kDa HA with the optimized siRNA (200 nM) and HA complexation conditions (64 μM). In this study, we evaluated two different siRNA molecules that target *STAT3*, and *glyceraldehyde 3-phosphate dehydrogenase* (*GAPDH*), a housekeeping gene. Quantitative RT-PCR analysis after 24-hours of transfection indicated that both 200 kDa and 300 kDa HA were functional in silencing target genes, *STAT3*, and *GAPDH* with 200 kDa marginally better than the 300 kDa (Figure 3b). These results also corroborate with our siRNA melting studies indicating a direct correlation between siRNA stabilization and transfection efficiency (Figure 1a).

To ascertain the CD44 dependence on the siRNA uptake and gene KD we performed CD44 receptor blocking studies.[11] In these experiments the plated MG-63 cells were first incubated with low molecular weight HA (5 kDa) for 2h and subsequently replenished with fresh medium containing 200 kDa HA (64 μM) and *anti-GAPDH* siRNA (200 nM). The medium was replaced with fresh medium after 5h and the KD was estimated by qRT-PCR experiment. The CD44 blocking and the subsequent gene silencing showed a significant reduction in target gene KD (from ~50% to 29% KD; Figure 3e). To probe the role of CD44 we performed the transfection experiment in low CD44 expressing human breast cancer cell line (MCF-7),[16] which demonstrated a modest 22% target gene KD. The CD44 blocking experiment in these cells resulted in a significant reduction in target gene KD (6%; Figure 3e). Our results clearly suggest the role of cell surface CD44 receptor in trafficking the siRNA across the cell membrane. The transfection efficiency was further evaluated at the protein levels by western blot analysis as well as by measuring the functional aspect of *STAT3* KD. Western blot results indicated that the HA-assisted transfection has led to significant downregulation of *STAT3* protein in MG-63 cells, although not as high as RNAiMAX (Figure 3f). Since functional KD of *STAT3* in MG-63 cells are known to induce apoptosis, we employed a commercially available triple detection assay (ApoTox-Glo™) to detect cell viability, cytotoxicity, and apoptosis aspects.[17] The transfection experiments after 3-days indicated upregulation of caspase-3/7 induced apoptosis in HA and RNAiMAX based transfection conditions, correlating with the qPCR and western blot results (Figure 3c). There were no significant differences between cell viability and cytotoxicity when 'scrambled' sequences were used, indicating that native HA, as well as RNAiMAX, are not toxic at the concentrations used.

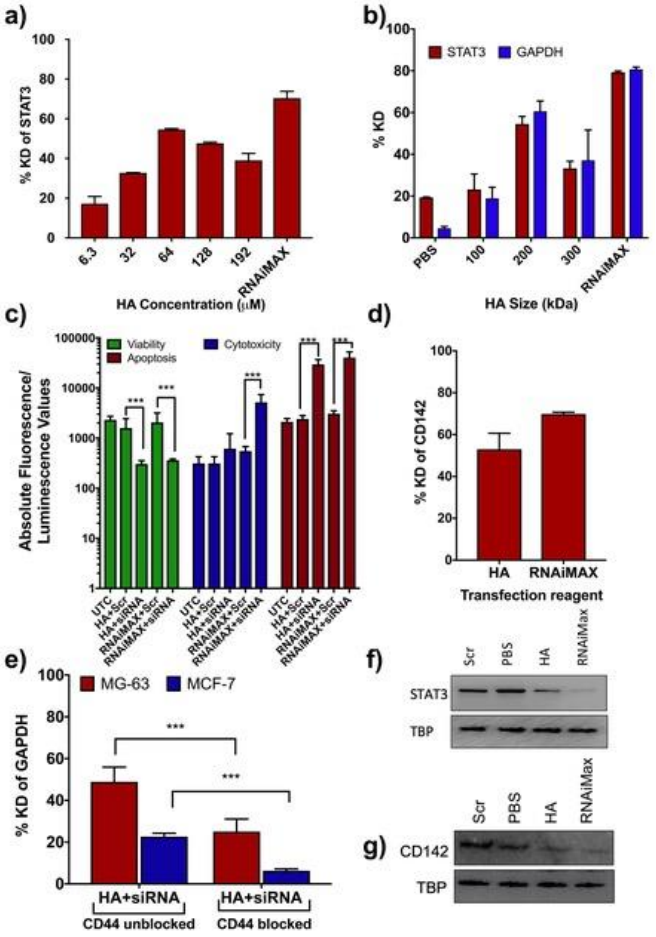

Figure 3. HA assisted RNAi in eukaryotic cells. **a)** HA concentration-dependent (6.3 – 198 μM) *in vitro* gene KD studies targeting the *STAT3* gene in human osteosarcoma cell line MG-63. **b)** HA size (100, 200, and 300 kDa; 64 μM) dependent *in vitro* KD studies targeting *STAT3* and *GAPDH* genes in MG-63 cells. RNAiMAX is used as a positive control. **c)** ApoTox-Glo™ assay is indicating cellular function after *STAT3* KD with HA and RNAiMAX as transfection reagents. Statistical analysis was performed using one-way ANOVA with Bonferroni's multiple comparison correction (***$p < 0.0001$). **d)** HA assisted KD studies for targeting tissue factor (CD142) gene. RNAiMAX is used as a positive control. **e)** CD44 blocking and its impact on target gene KD in MG-63 and MCF-7 cell lines. **f)** Western blot analysis *in vitro* KD of *STAT3* protein in MG-63 cells. RNAiMAX is used as a positive control for transfection. **g)** Western blot analysis *in vitro* KD of CD142 protein in MG-63 cells. RNAiMAX is used as a positive control for transfection. TATA box-binding protein (TBP) is used as an internal control for western blot analysis.

Because HA-based delivery of nucleic acids is particularly interesting for stem cells (such as primary human mesenchymal stem/stromal cells (MSCs) as it expresses several HA-specific receptors on the cell surface such as CD44, CD54, and CD168.[18] Thus, several groups have developed HA-cationic polymer conjugates and demonstrated siRNA delivery in MSCs.[19] We, therefore, tested our anionic delivery strategy on MSCs and targeted the pro-coagulant target namely *tissue factor-III*, also known as CD142. Suppression of CD142 will significantly improve the MSCs survival upon transplantation, which remains as one of the major challenges in the field. The quantitative RT-PCR evaluation indicated that HA assisted delivery of *anti-CD142* siRNA resulted in 50% gene KD as anticipated (Figure 3d). Our positive control experiment using RNAiMAX resulted in nearly 70% KD. Further analysis at the post-translational level after 48 h using western blot analysis indicated that the HA-assisted delivery of *anti-CD142* siRNA to hMSCs significantly downregulated the target gene when compared to the 'scrambled' and untreated controls (Figure 3g). The level of protein KD was almost identical to the RNAiMAX assisted transfection.

In conclusion, we present the first evidence that native extracellular biopolymer, namely HA, stabilize nucleic acids by hydrogen bonds as well as by hydrophobic interactions. Such stabilization was evident by thermal melting experiments, gel shift assay, light scattering, scanning electron microscopy as well as computational methods. We further demonstrated that such interactions could be used to deliver functional siRNA in CD44 positive cancer cells as well as primary cells without inducing any toxicity. Our results present a new insight on the role of extracellular matrix in trafficking nucleic acids, which presumably happen naturally *in vivo*. We believe our results will broaden the understanding of the role of ECM in RNA biology and enable development of novel non-cationic, non-viral delivery strategies for therapeutic nucleic acids.

Acknowledgements

We would like to thank Prof. Martin J. Stoddart from AO Research Institute Davos, Switzerland for gifting us primary human MSCs and Michela Castelnuovo, B. Des. for image editing. We acknowledge financial support from Swedish Strategic Research 'StemTherapy' (Dnr 2009-1035); European Union's Seventh Framework Programme FP7/2007-2013/607868 (Marie Curie Actions- iTERM) and Swedish foundation for strategic research (SSF, SBE13-0028). We also acknowledge the contribution of the computational resources provided by Euler Cluster of ETH Zürich and Tampere Imaging Facility (TIF), Finland for their service.

Conflict of interest

The authors declare no conflict of interest.

Keywords: Hyaluronic acid • Transfection • RNAi • Delivery • Extracellular matrix

[1] J. E. Freedman *et al. Nat. Commun.* **2016**, *7*, 11106.
[2] P. Mandel, P. Metais, *C R Acad. Sci. Paris* **1948**, *142*, 241-243.
[3] a) J. D. Arroyo, J. R. Chevillet, E. M. Kroh, I. K. Ruf, C. C. Pritchard, D. F. Gibson, P. S. Mitchell, C. F. Bennett, E. L. Pogosova-Agadjanyan, D. L. Stirewalt, J. F. Tait, M. Tewari, *Proc. Natl. Acad. Sci. U.S.A.* **2011**, *108*, 5003-5008; b) A. Turchinovich, L. Weiz, A. Langheinz, B. Burwinkel, *Nucleic Acids Res.* **2011**, *39*, 7223-7233; c) K. C. Vickers, B. T. Palmisano, B. M. Shoucri, R. D. Shamburek, A. T. Remaley, *Nat Cell Biol* **2011**, *13*, 423-433; d) L. Li, D. Zhu, L. Huang, J. Zhang, Z. Bian, X. Chen, Y. Liu, C. Y. Zhang, K. Zen, *PLoS One* **2012**, *7*, e46957.
[4] M. A. Cortez, C. Bueso-Ramos, J. Ferdin, G. Lopez-Berestein, A. K. Sood, G. A. Calin, *Nat. Rev. Clin. Oncol.* **2011**, *8*, 467.
[5] N. B. Tsui, E. K. Ng, Y. M. Lo, *Clin. Chem.* **2002**, *48*, 1647-1653.
[6] R. Lucas, I. Gómez-Pinto, A. Aviñó, J. J. Reina, R. Eritja, C. González, J. C. Morales, *J. Am. Chem. Soc.* **2011**, *133*, 1909-1916.
[7] E. M. Munoz, M. Lopez de la Paz, J. Jimenez-Barbero, G. Ellis, M. Perez, C. Vicent, *Chem. Eur. J.* **2002**, *8*, 1908-1914.
[8] M. J. Han, K. S. Yoo, K. H. Kim, G. H. Lee, J. Y. Chang, *Macromolecules* **1997**, *30*, 5408-5415.
[9] O. P. Varghese, W. Sun, J. Hilborn, D. A. Ossipov, *J. Am. Chem. Soc.* **2009**, *131*, 8781-8783.
[10] H. J. Yan, T. Casalini, G. Hulsart-Billstrom, S. Wang, O. P. Oommen, M. Salvalaglio, S. Larsson, J. Hilborn, O. P. Varghese, *Biomaterials* **2018**, *161*, 190-202.
[11] O. P. Oommen, C. Duehrkop, B. Nilsson, J. Hilborn, O. P. Varghese, *ACS Appl. Mater. Interfaces* **2016**, *8*, 20614-20624.
[12] Y. Hongji, O. O. P., Y. Di, H. Jöns, Q. Hong, V. O. P., *Adv. Funct. Mater.* **2015**, *25*, 3907-3915.
[13] K. Hosono, Y. Nishida, W. Knudson, C. B. Knudson, T. Naruse, Y. Suzuki, N. Ishiguro, *Am. J. Pathol.* **2007**, *171*, 274-286.
[14] M. Z. Kamran, P. Patil, R. P. Gude, *Biomed. Res. Int.* **2013**, *2013*, 421821.
[15] D. Hong *et al. Sci. Transl. Med.* **2015**, *7*, 314ra185.
[16] O. P. Oommen, J. Garousi, M. Sloff, O. P. Varghese, *Macromol. Biosci.* **2014**, *14*, 327-333.
[17] L. H. Liu, H. Li, J. P. Li, H. Zhong, H. C. Zhang, J. Chen, T. Xiao, *Biochem. Biophys. Res. Commun.* **2011**, *416*, 31-38.
[18] L. Bian, M. Guvendiren, R. L. Mauck, J. A. Burdick, *Proc. Natl. Acad. Sci. U.S.A.* **2013**, *110*, 10117-10122.
[19] a) H. Yang *et al. Eur. J. Pharm. Sci.* **2014**, *53*, 35-44; b) G. Jiang, K. Park, J. Kim, K. S. Kim, S. K. Hahn, *Mol. Pharm.* **2009**, *6*, 727-737.